Direct and precise mapping of intramolecular H-atom motion in H_2 by an electron-atom Compton scattering experiment

Yuichi Tachibana,[1] Yuuki Onitsuka,[1] Hirohiko Kono,[2] and Masahiko Takahashi[1,*]
[1] *Institute of Multidisciplinary Research for Advanced Materials, Tohoku University, Sendai 980-8577, Japan*
[2] *Department of Chemistry, Graduate School of Science, Tohoku University, Sendai 980-8578, Japan*

(Received 16 April 2022; accepted 16 May 2022; published 31 May 2022)

We report an electron-atom Compton scattering experiment on the H_2 molecule. The momentum distribution of the H atom due to intramolecular motion was obtained by using a protocol developed for the data analysis. Furthermore, it is shown that the experimental result agrees well with associated calculations based on quantum chemistry theory. This indicates not only the validity of the protocol but also the feasibility of use of the experiment as an unconventional molecular spectroscopy, opening the door to direct and precise mapping of intramolecular motion of each atom with different masses.

DOI: 10.1103/PhysRevA.105.052813

I. INTRODUCTION

The individual atoms of a molecule are not at rest but are moving even at zero temperature. Since such atomic motions often govern various properties of molecules, they have long been attracting a great deal of attention from a diverse field that spans a broad range of research areas and applications. The technique most widely used for the study is vibrational spectroscopy, which measures frequencies of normal modes represented by an orthogonal set of harmonic oscillators [1]. Illustrative examples of its great analytical power can be found a lot in literature, particularly when applied to relatively small molecules, because the vibrational frequencies act as a fingerprint of the molecular structure and its structural change [2]. It should be noted, however, that with the increase in the molecular size, many of the normal modes will have very similar frequencies and are eventually no longer distinguishable from one another. In other words, normal modes often include collective motion of many (or all) of the constituent atoms, and hence the displacement of an atom is observed only in the form of a linear combination of normal modes [3,4]. As a result, vibrational spectroscopy on such large molecules is usually limited to identifying frequencies associated with specific groups of atoms within the molecule, i.e., functional groups. Keeping in mind that chemistry is local owing to the short-range nature of chemical forces and an atom sees only its immediate surroundings [5], one may desire to have an experimental technique to map each atomic motion or to decompose the collective-atomic-motion description into the most elementary components.

An electron-atom Compton scattering experiment, also known as atomic momentum spectroscopy (AMS) [6], is a method that inherently possesses the ability to map intramolecular motion of each atom with different masses. Despite the abundance of the previous works [7–12], however, no measurement has been reported, which has observed atomic momentum distribution due only to intramolecular motion. The material reason behind this situation is that there is no general protocol for the data analysis. Basically, AMS experimental raw data are inextricably composed of four types of contributions: (i) instrumental response (IR) function, (ii) molecular center-of-mass translational motion, (iii) molecular vibration, and (iv) molecular rotation. In the absence of the general protocol, for instance, our latest work on H_2 and D_2 [12] was able to access the intramolecular atomic motion only through curve fitting to the experimental data using a trial function based on the theoretical prediction of the harmonic oscillator model [13], even when the contribution of molecular rotation was assumed to be negligibly small.

In this paper we propose a complete set of data-analysis protocol to extract atomic momentum distribution due only to intramolecular motion from AMS experimental raw data or to exclude effects of molecular translational motion and IR function. Note that the word "intramolecular" is used here so that it includes both molecular vibration and rotation, as rotational motion is essentially inseparable from vibrational motion without imposing the Eckart frame on the Schrödinger equation [1,14]. The most significant value of the protocol lies in its applicability that works generally for any kind of molecular systems involving polyatomic transient species; no knowledge about the functional form of the atomic momentum distribution is required. The validity of the general protocol is demonstrated by comparing an experimental result obtained for the H-atom motion in H_2 with associated quantum chemistry-based calculations.

II. EXPERIMENT AND DATA ANALYSIS

Within the plane-wave impulse approximation [8,15], the AMS scattering by a molecule can be described as a billiard-ball-type collision of the incident electron with a constituent atom. Namely, the scattering atom is treated as a "single" free particle so that it absorbs all of the momentum transfer $\boldsymbol{K}$

---

[*] masahiko@tohoku.ac.jp

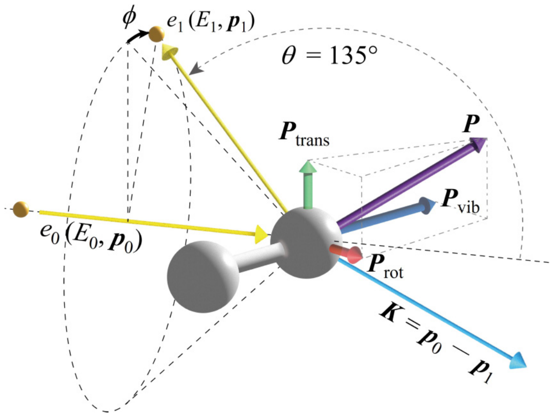

FIG. 1. Kinematics of electron-atom Compton scattering.

(=$\boldsymbol{p}_0$–$\boldsymbol{p}_1$) with $\boldsymbol{p}_j$'s ($j = 0, 1$) being the momenta of the incident and quasielastically backscattered electrons. The energy loss $E_{\rm loss}$ (=E_0–E_1) of the incident electron, produced by the collision with the scattering atom having mass $M_{\rm sc}$ and initial momentum $\boldsymbol{P}$, is then given by

$$E_{\rm loss} = \frac{(\boldsymbol{P}+\boldsymbol{K})^2}{2M_{\rm sc}} - \frac{P^2}{2M_{\rm sc}} = \frac{K^2}{2M_{\rm sc}} + \frac{\boldsymbol{P}\cdot\boldsymbol{K}}{M_{\rm sc}}. \quad (1)$$

Here the first term in the rightmost side of Eq. (1) is a function of $M_{\rm sc}$ and it represents the mean recoil energy $\bar{E}_{\rm recoil}$ that corresponds to the recoil with the scattering atom being stationary ($\boldsymbol{P} = 0$). The second term is the Doppler broadening caused by the initial momentum of the scattering atom motion, which is the sum of the momenta due to molecular translational motion ($\boldsymbol{P}_{\rm trans}$), molecular vibration ($\boldsymbol{P}_{\rm vib}$), and molecular rotation ($\boldsymbol{P}_{\rm rot}$), as shown in Fig. 1. Energy analysis of the scattered electrons can thus provide direct information about $\boldsymbol{P}$ in the form of $\boldsymbol{P}\cdot\boldsymbol{K}$. In addition, since gaseous H_2 molecules employed in the present study were randomly oriented in space, what the AMS experiment measured is spherically averaged atomic momentum distribution.

The AMS experiment on H_2 was carried out at an incident electron energy of 2.0 keV by using a multichannel spectrometer. Since details of the spectrometer are described elsewhere [16], a brief account of it is given here. A thermal electron gun generated an incident electron beam with intensity of a few hundred nanoamperes. Quasielastic electron backscattering occurred where the incident electron beam collided with a gaseous H_2 molecule in an effusive beam. Here a high-purity (>99.999 99%) H_2 gas was obtained from Taiyo Nippon Sanso Corporation and used at room temperature. A spherical analyzer accepted the scattered electrons emerging at a scattering angle of $\theta = 135° \pm 0.4°$ ($K = 22.4$ a.u.) over azimuthal-angle (ϕ) ranges from 0° to 72.5°, from 107.5° to 252.5°, and from 287.5° to 360°. The electrons passing through the analyzer were detected with a position-sensitive detector. The experimental raw data were eventually obtained by subtracting the spectra measured at an ambient pressure of 1.0×10^{-5} Pa in the vacuum chamber from those at 2.5×10^{-4} Pa to remove unexpected background signals. The resulting instrumental energy resolution was ~0.6 eV full width at half maximum. An additional AMS experiment was also conducted for Kr to estimate the IR function [11], as Kr is a heavy atom and it does not have intramolecular motion while its $\bar{E}_{\rm recoil}$ value can be regarded as zero under the experimental conditions employed.

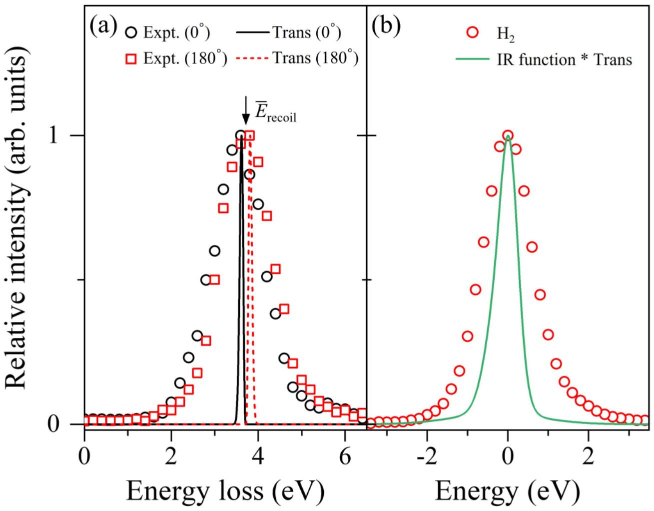

FIG. 2. (a) Comparison of EEL spectra measured for H_2 at $\phi = 0°$ and 180°. The solid and dashed lines represent associated theoretical calculations for the Doppler broadening due to molecular translational motion at $\phi = 0°$ and 180°, respectively. (b) A ϕ-angle integrated energy spectrum of H_2 created by summing up the aligned EEL spectra at each ϕ. The solid line shows the practical IR function (IR function $*$ Trans). See text for details.

The general protocol developed for mapping atomic momentum distribution due only to intramolecular motion involves the following three steps. Firstly, the effect of molecular translational motion needs to be considered. To illustrate it, Fig. 2(a) compares electron-energy-loss (EEL) spectra measured for H_2 at $\phi = 0°$ and 180°. It is evident that peak positions of the two bands are different from each other. The energy difference between the two originates in exactly the effect of molecular translational motion, as reported in our previous study [12] in which the ϕ-angle dependence of the peak positions is found to be reproduced well by our gas beam model [11] using the most probable velocity $v_{\rm mp} = \sqrt{3k_BT/M_{H_2}}$ with $k_{\rm B}$, T, and M_{H_2} being the Boltzmann constant, temperature, and mass of the H_2 molecule. The Doppler broadening spectra of translational motion, predicted by the gas beam model, are also shown in Fig. 2(a). Clearly, their widths are much smaller compared to the observed band widths. In this way, translational motion of molecules in the effusive beam experiment has a similar effect to the Dirac delta function, which shifts EEL spectra at each ϕ to higher or lower energy loss with respect to $\bar{E}_{\rm recoil}$, while keeping their band shapes unchanged [11,12]. Secondly, both the energy shifts due to $\bar{E}_{\rm recoil}$ and translational motion should be canceled out. This can be done by aligning the band peak positions of the EEL spectra at each ϕ to the origin of the energy axis. Figure 2(b) shows a ϕ-angle integrated energy spectrum of H_2, which has been created by summing up the aligned EEL spectra at each ϕ. Also included in the figure is a convolution of the aligned Doppler broadening spectrum of translational motion and the IR function, the latter of which can be approximated as an aligned EEL spectrum of Kr [11].

The convolution curve should be employed as the practical IR function in the H_2 data analysis. Lastly, contribution of intramolecular atomic motion has to be separated from that of the practical IR function. Use of the convolution theorem [17] is best suited for this purpose. Since Fourier transform (FT) of the convolution of two functions is the product of FTs of each function, intramolecular atomic momentum distribution can be obtained by dividing the FT of the experiment by that of the practical IR function and then taking the inverse FT of the result of the division. It should be noted that this general protocol enables one to apply the convolution theorem simultaneously to multiple bands for heteronuclear molecules, in addition to no requirement of knowledge about the functional form of the atomic momentum distribution in question. Application of the general protocol to polyatomic molecules such as CH_4 will be reported elsewhere.

III. THEORY

Quantum chemistry-based calculations have also been performed to have a reference standard for evaluating the quality of the general protocol. In the calculations, a wave function $\Psi(\boldsymbol{R}_1, \boldsymbol{R}_2)$ was employed to describe the nuclear motion of the H_2 molecule, which is given by

$$\Psi(\boldsymbol{R}_1,\boldsymbol{R}_2)=\left(\frac{2\gamma}{\pi}\right)^{3/4}\exp\left[-\gamma\left(\frac{\boldsymbol{R}_1+\boldsymbol{R}_2}{2}\right)^2\right] \times\frac{f(R-R_\mathrm{e})}{R}Y_{JM}(\hat{R}). \qquad (2)$$

Here $\boldsymbol{R}_j$ $(j = 1, 2)$ is the jth atom position. R and R_e are the internuclear distance ($|\boldsymbol{R}_1–\boldsymbol{R}_2|$) and its equilibrium value. γ is a parameter for the width of a wave packet to represent the molecular center-of-mass motion. $f(R–R_\mathrm{e})$ is the vibrational wave function and at room temperature it can be approximated as a ground-state wave function, $(\mu\omega/\pi\hbar)^{1/4}\exp[-\mu\omega(R–R_\mathrm{e})^2/2\hbar]$ with μ, ω, and $\hbar$ being the reduced mass, angular frequency, and reduced Planck's constant. Y_{JM} is the spherical harmonics with rotational quantum number J and magnetic quantum number M. By taking the FT of $\Psi(\boldsymbol{R}_1, \boldsymbol{R}_2)$ to have $\Psi(\boldsymbol{P}_1, \boldsymbol{P}_2)$ and taking the limit of the integral of $|\Psi(\boldsymbol{P}_1, \boldsymbol{P}_2)|^2$ over $\boldsymbol{P}_2$ as γ approaches zero, $|\Psi(\boldsymbol{P}_1)|^2$ is obtained as follows:

$$\begin{aligned}|\Psi(\boldsymbol{P}_1)|^2 &= \lim_{\gamma\to 0}\int|\Psi(\boldsymbol{P}_1,\boldsymbol{P}_2)|^2 d\boldsymbol{P}_2\\ &=\left(\frac{2}{\pi}\right)Y^*_{JM}(\hat{\boldsymbol{P}}_1)Y_{JM}(\hat{\boldsymbol{P}}_1)\\ &\quad\times\left|\int j_J(P_1R)f(R-R_\mathrm{e})R\,dR\right|^2, \end{aligned}\qquad (3)$$

where $j_J(P_1R)$ is the spherical Bessel function of order J. Since rotational states with the same J number but different M numbers are equally populated in the experiment, summation of $|\Psi(\boldsymbol{P}_1)|^2$ should be made over the M numbers:

$$\sum_{M=-J}^{+J}|\Psi(\boldsymbol{P}_1)|^2=\left(\frac{2J+1}{2\pi^2}\right)\left|\int j_J(P_1R)f(R-R_\mathrm{e})R\,dR\right|^2. \qquad (4)$$

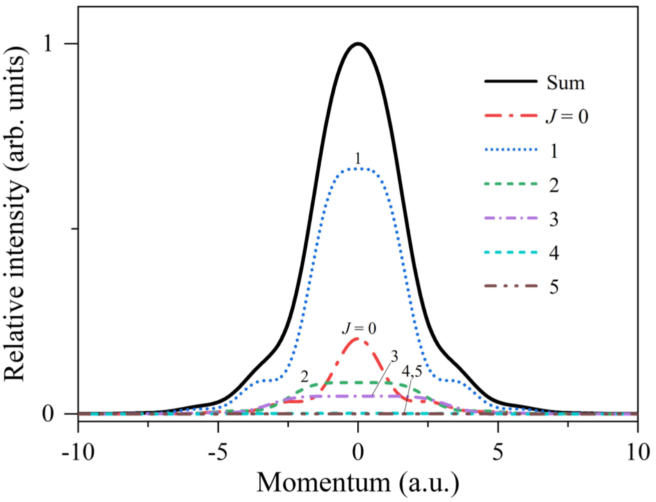

FIG. 3. A theoretical AMS spectrum due to intramolecular H-atom motion in H_2 (Sum) and its components with rotational quantum number of J up to 5.

Note that the summation yields an isotropic functional form and $\sum_M|\Psi(\boldsymbol{P}_1)|^2$ corresponds to atomic momentum distribution $[\rho_J(\boldsymbol{P}_1)]$ of a spherically averaged H_2 molecule in the rotational state with a J number. On the other hand, the relative populations of rotational states with different J numbers are temperature dependent and they can be taken into account by using the Boltzmann distribution function. Keeping in mind also that AMS measures the sum of projections of each $\rho_J(\boldsymbol{P}_1)$ onto $\hat{\boldsymbol{K}}$, one has the following expression for $\rho_\mathrm{AMS}(P_1^K)$ which can directly be compared with the experiment:

$$\rho_\mathrm{AMS}(P_1^K)\propto\sum_{J=0}^{\infty}g_\mathrm{ns}\exp\left[-\frac{BJ(J+1)}{k_BT}\right] \times\int\rho_J(\boldsymbol{P}_1)d\boldsymbol{P}_1\delta(\boldsymbol{P}_1\cdot\hat{\boldsymbol{K}}-P_1^K). \qquad (5)$$

Here g_ns is the nuclear spin degeneracy and $g_\mathrm{ns} = 1$ for even and 3 for odd J. B is the rotational constant and $B = 60.853\,\mathrm{cm}^{-1}$ [18] was employed in the present calculations. The calculated J components and their sum $[\rho_\mathrm{AMS}(P_1^K)]$ are shown in Fig. 3. The spectrum of $\rho_\mathrm{AMS}(P_1^K)$ is referred to as the AMS spectrum hereafter.

IV. RESULTS AND DISCUSSION

Figure 4 compares the experimental AMS spectrum thus obtained for H_2 by using the general protocol with the quantum chemistry-based calculations. Also included in the figure is another theoretical AMS spectrum, generated by using the classical kinetic energy model [19] that was often employed in the earlier AMS studies. It is evident, on one hand, that the classical model calculations fail to quantitatively reproduce the experiment. On the other hand, a good agreement between the experiment and quantum chemistry calculations is demonstrated for the intramolecular H-atom motion in H_2. This observation indicates not only the validity of our proposed general protocol but also the feasibility of use of AMS

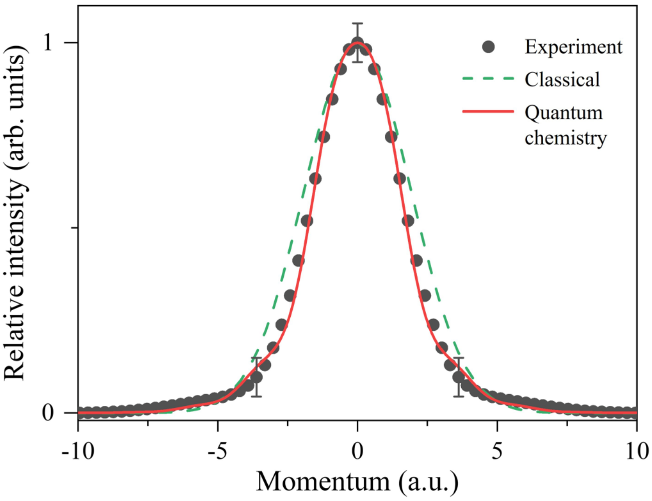

FIG. 4. Comparison between experiment and theory for the AMS spectrum due to intramolecular H-atom motion in H_2. The solid and dashed lines represent theoretical spectra generated by using quantum chemistry theory and the classical kinetic energy model, respectively.

experiment as an unconventional molecular spectroscopy, opening the door to direct and precise mapping of intramolecular motion of each atom with different masses. Note that neutron Compton scattering [20] can provide the same information. However, it has been employed for solids, but has never been applied to low density targets such as gaseous molecules due to the weak interaction with matter. In this regard, AMS is unique in its ability to be used as a molecular spectroscopy. The unique ability of AMS should be applied to have a basic understanding, from different perspectives, of the static and dynamic behavior of various molecules in various environments such as gaseous molecules, molecules adsorbed on surfaces, and transient, evolving systems during chemical reaction. For instance, consider a case in which a H_2 molecule starts to dissociate into two H atoms along the $\boldsymbol{K}$ direction. In this case, the two atoms move to the opposite direction from each other, so the AMS spectrum of the dissociating H_2 molecule splits from one band into two bands and eventually those with a momentum separation determined by the kinetic energy release. Here Ehrenfest's theorem, which relates the time derivative of the expectation value of the momentum operator $\boldsymbol{P}$ to the expectation value of the force, guarantees that time-resolved versions of AMS experiments would provide a real-time measure of the intramolecular force acting on each atom with different masses. In this manner, the time evolution of the AMS spectrum for a transient species is expected to provide a wealth of information on the relevant potential energy surface. Our future efforts will be directed along this line also [21].

ACKNOWLEDGMENTS

This work was partially supported by the JSPS KAKENHI Grants No. 20J12788, No. 21H04672, and No. 21K18926. This work was also supported in part by "Five-star Alliance."

---

[1] E. B. Wilson, Jr., J. C. Decius, and P. C. Cross, *Molecular Vibrations: The Theory of Infrared and Raman Vibrational Spectra* (Dover, New York, 1980).
[2] E. T. J. Nibbering, H. Fidder, and E. Pines, Annu. Rev. Phys. Chem. **56**, 337 (2005).
[3] X. Cheng and R. P. Steele, J. Chem. Phys. **141**, 104105 (2014).
[4] R. C. Couto, V. V. Cruz, E. Ertan, S. Eckert, M. Fondell, M. Dantz, B. Kennedy, T. Schmitt, A. Pietzsch, F. F. Guimarães, H. Ågren, F. Gel'mukhanov, M. Odelius, V. Kimberg, and A. Föhlisch, Nat. Commun. **8**, 14165 (2017).
[5] R. D. Levine, *Molecular Reaction Dynamics* (Cambridge University Press, Cambridge, 2005).
[6] M. Vos, Phys. Rev. A **65**, 012703 (2001).
[7] M. Vos and M. R. Went, J. Phys. B: At., Mol. Opt. Phys. **42**, 065204 (2009).
[8] M. Vos, J. Chem. Phys. **132**, 074306 (2010).
[9] M. Vos, E. Weigold, and R. Moreh, J. Chem. Phys. **138**, 044307 (2013).
[10] M. Vos, J. Phys. B: At., Mol. Opt. Phys. **49**, 145202 (2016).
[11] M. Yamazaki, Y. Tachibana, and M. Takahashi, J. Phys. B: At., Mol. Opt. Phys. **52**, 65205 (2019).
[12] Y. Tachibana, M. Yamazaki, and M. Takahashi, Phys. Rev. A **100**, 032506 (2019).
[13] E. B. Karlsson, Nucl. Instrum. Methods Phys. Res., Sect. A **694**, 286 (2012).
[14] C. Eckart, Phys. Rev. **47**, 552 (1935).
[15] V. F. Sears, Phys. Rev. B **30**, 44 (1984).
[16] M. Yamazaki, M. Hosono, Y. Tang, and M. Takahashi, Rev. Sci. Instrum. **88**, 063103 (2017).
[17] W. H. Press, S. A. Teukolsky, W. T. Vetterling, and B. P. Flannery, *Numerical Recipes in C: The Art of Scientific Computing,* 2nd ed. (Cambridge University Press, New York, 1992).
[18] K. P. Huber and G. Herzberg, *Molecular Spectra and Molecular Structure IV. Constants of Diatomic Molecules* (Van Nostrand Reinhold, New York, 1979).
[19] R. Moreh and D. Nemirovsky, J. Chem. Phys. **133**, 084506 (2010).
[20] G. I. Watson, J. Phys.: Condens. Matter **8**, 5955 (1996).
[21] Y. Tachibana, Y. Onitsuka, M. Yamazaki, and M. Takahashi, Atoms **9**, 19 (2021).